Theory of integer quantum Hall effect in graphene

Igor F. Herbut
Department of Physics, Simon Fraser University, Burnaby, British Columbia, Canada V5A 1S6
(Received 5 January 2007; published 18 April 2007)

The observed quantization of the Hall conductivity in graphene at high magnetic fields is explained as being due to the dynamically generated spatial modulation of either the electron spin or the density, as decided by the details of Coulomb interaction on the scale of lattice constant. It is predicted that at a large in-plane component of the magnetic field such ordering may be present only at the filling factor $f=\pm 1$ and absent otherwise. Other experimental consequences of the theory are outlined.

DOI: 10.1103/PhysRevB.75.165411 PACS number(s): 73.43.−f, 71.10.Fd, 71.10.Pm, 71.70.Di

Graphene is a two-dimensional semimetal with gapless Dirac-like excitations near two points in the Brillouin zone.[1,2] When placed in the uniform magnetic field of several tesla, it exhibits plateaus in the Hall conductivity at integer filling factors $f=4n+2$,[3,4] just as implied by the Landau-level (LL) spectrum of the single-particle Dirac equation,[5] with each LL being fourfold degenerate in spin and sublattice indices. Although the strength of the Coulomb interaction between the conducting electrons in graphene is similar to the bandwidth, the semimetallic ground state at zero magnetic field indicates that it is below the critical value needed for insulation.[6,7]

At magnetic fields above ~ 10 T, however, additional quantum Hall (QH) states at $f=0,\pm 1,\pm 4$ appear.[8] Plateaus in the Hall conductivity at other integers, such as at $f=\pm 3$ or $f=\pm 5$, for example, are at the same time conspicuously absent, even at the highest magnetic field of 45 T. The experiment[8] also suggests that the activation gaps at $f=\pm 4$ are likely to be due to the Zeeman splitting of the first LL. The quantization at $f=\pm 1$, however, implies that the fourfold degeneracy of the zeroth LL has been completely lifted, which calls for the inclusion of the Coulomb interactions into consideration. The theory of the integer QH effect in graphene would thus have at least to provide answers to the following questions: (a) why has the fourfold degeneracy of *only* the $n=0$ LL been completely lifted at the magnetic fields and samples under study, (b) why do new incompressible states at $f=0,\pm 1,\pm 4$ require higher magnetic fields to appear than those at $f=4n+2$, and finally, (c) what is the nature of the interacting ground states at different filling factors?

The first question may be immediately answered by postulating that the Dirac fermions have acquired an effective gap in a form of a "relativistic mass" due to the Coulomb interaction.[9] Such a gap reduces the degeneracy of *only* the zeroth LL. Including the Zeeman splitting then leads to the spectrum of the effective single-particle Hamiltonian precisely as required by the observed pattern of quantization of Hall conductivity. It is unclear, however, under which circumstances and which one of the multitude of such gaps that could exist, as discussed below, is generated dynamically. This problem is addressed here within the extended Hubbard model on a honeycomb lattice, with both on-site and nearest-neighbor repulsions. This is the simplest Hamiltonian that mimics the effect of Coulomb repulsion and which contains the possibilities of charge-density-wave (CDW) and antiferromagnetic (AF) orders. Previous work indicated[7,10] that these two are in direct competition at zero magnetic field and when the interaction is strong. Here we solve the model in the physical *weak*-coupling regime and in an external magnetic field, allowing only for the simplest AF state with the staggered magnetization parallel to the magnetic field. The results are summarized as the phase diagrams in Figs. 1 and 2. At half-filling and for a weak enough Zeeman energy the system could be either a CDW or an AF, depending on which coupling dominates (Fig. 2). For a larger Zeeman energy the ground state at $f=0$ becomes magnetic with full lattice symmetry. Nevertheless, even in the latter case increasing the chemical potential produces an incompressible state at $f=1$, with the activation gap becoming equal to the "relativistic" gap (Fig. 1). In contrast, at weak Zeeman coupling we find a direct transition between $f=0$ and $f=2$ states. At $f\geqslant 2$ the relativistic gap vanishes. Experiments that would test the presented against other theories[12–15] are discussed.

We define the extended Hubbard model as $H=H_0+H_1$, where

$$H_0=-t\sum_{\vec{A},i,\sigma=\pm} u_\sigma^\dagger(\vec{A})v_\sigma(\vec{A}+\vec{b}_i)+\text{H.c.}, \tag{1}$$

$$H_1=U\sum_{\vec{X}} n_+(\vec{X})n_-(\vec{X})+\frac{V}{2}\sum_{\vec{A},i,\sigma,\sigma'} n_\sigma(\vec{A})n_{\sigma'}(\vec{A}+\vec{b}_i). \tag{2}$$

The sites $\vec{A}$ denote one triangular sublattice of the honeycomb lattice, generated by linear combinations of the basis vectors $\vec{a}_1=(\sqrt{3},-1)(a/2)$ and $\vec{a}_2=(0,a)$. The second sublattice is then at $\vec{B}=\vec{A}+\vec{b}$, with the vector $\vec{b}$ being either $\vec{b}_1=(1/\sqrt{3},1)(a/2)$, $\vec{b}_2=(1/\sqrt{3},-1)(a/2)$, or $\vec{b}_3=(-a/\sqrt{3},0)$. $a\approx 2.5A$ is the lattice spacing, and $t\approx 2.5$ eV, $U\approx 5-12$ eV, and $U/V\approx 2-3$.[10]

The spectrum of H_0 becomes linear in the vicinity of the two Dirac points at $\pm\vec{K}$, with $\vec{K}=(1,1/\sqrt{3})(2\pi/a\sqrt{3})$.[1,2] Retaining only the Fourier components near $\pm\vec{K}$ one can write, in continuum notation,

$$H_0=\int d\vec{x}\sum_\sigma \Psi_\sigma^\dagger(\vec{x})i\gamma_0\gamma_i D_i\Psi_\sigma(\vec{x}) \tag{3}$$

and

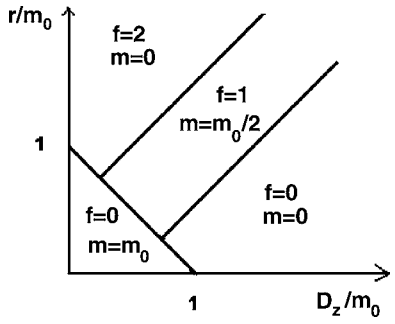

FIG. 1. The proposed phase diagram of graphene in the magnetic field. $D_z=g_zB$ is the Zeeman energy, r is the chemical potential, and $m_0=2g_xB_\perp/\pi$ is the characteristic size of the "relativistic" many-body gap m. g_x is the larger of the couplings in the CDW and AF channels (see the text).

$$\Psi_\sigma^\dagger(\vec{x}) = \int^\Lambda \frac{d\vec{q}}{(2\pi a)^2} e^{-i\vec{q}\cdot\vec{x}}[u_\sigma^\dagger(\vec{K}+\vec{q}), v_\sigma^\dagger(\vec{K}+\vec{q}), u_\sigma^\dagger(-\vec{K}+\vec{q}), v_\sigma^\dagger(-\vec{K}+\vec{q})], \tag{4}$$

$i=1,2$, where it was convenient to rotate the reference frame so that $q_1=\vec{q}\cdot\vec{K}/K$ and $q_2=(\vec{K}\times\vec{q})\times\vec{K}/K^2$, and set $\hbar=e/c=v_F=1$, where $v_F=ta\sqrt{3}/2$ is the Fermi velocity. Here $i\gamma_0\gamma_1=\sigma_z\otimes\sigma_x$, $i\gamma_0\gamma_2=-I_2\otimes\sigma_y$, with I_2 as the 2×2 unit matrix and $\vec{\sigma}$ as the Pauli matrices. $\Lambda\approx1/a$ is the ultraviolet cutoff over which the linear approximation for the dispersion holds. The orbital effect of the magnetic field is included by defining $D_i=-i\partial_i-A_i$, with its component perpendicular to the graphene's plane being $B_\perp=\partial_1A_2-\partial_2A_1$.

Consider an auxiliary single-particle Hamiltonian $\tilde{H}$:

$$\tilde{H} = mM + i\gamma_0\gamma_iD_i, \tag{5}$$

where M is a Hermitian 4×4 matrix. When $m=0$, $\tilde{H}=H_0$, for each spin state. Also, if $M^2-1=\{M,\gamma_0\gamma_i\}=0$,

$$\tilde{H}^2 = D_i^2 + B(\sigma_z\otimes\sigma_z) + m^2. \tag{6}$$

This is the case if either

$$M = M_1 = a(I_2\otimes\sigma_z) + b(\sigma_x\otimes\sigma_x) + c(\sigma_y\otimes\sigma_x) \tag{7}$$

with real a,b,c, which satisfy $a^2+b^2+c^2=1$, or

$$M = M_2 = \sigma_z\otimes\sigma_z. \tag{8}$$

In either case the eigenvalues of $\tilde{H}^2$ are at $2nB+m^2$, with $n=0,1,2,\ldots$. For $n>0$ this immediately implies that eigenvalues of $\tilde{H}$ itself are at $\pm\sqrt{2nB+m^2}$, with the degeneracies of B/π per unit area being the same as for $m=0$. For $n=0$, on the other hand, an elementary calculation gives that the eigenvalues of $\tilde{H}$, (a) for any M_1, are at $\pm|m|$, each with halved degeneracy of $B/2\pi$ (per unit area), and (b) for M_2, are at m, still with the full degeneracy of B/π. The invariance of the spectrum in the first case under rotations of the unit vector (a,b,c) is the consequence of the "chiral" SU(2) symmetry of H_0 generated by $\{\gamma_{35},\gamma_3,\gamma_5\}$, where $\gamma_3=\sigma_x\otimes\sigma_y$, $\gamma_5=\sigma_y\otimes\sigma_y$, and $\gamma_{35}=i\gamma_3\gamma_5$, for example.[7,11] Any specific choice of M_1 in $\tilde{H}$ breaks this SU(2) down to U(1) and leads to the same eigenvalues. M_2 preserves the chiral symmetry and hence implies a different spectrum.

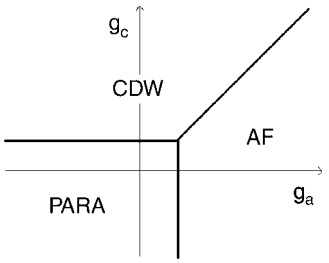

FIG. 2. The phase diagram at half-filling ($r=0$). The translationally symmetric magnet exists for $g_c,g_a<\pi g_zB/2B_\perp$.

Assuming that such an effective chiral-symmetry-breaking gap m becomes generated by interactions and then splitting the resulting energy levels further by the standard Zeeman effect could thus lead to the QH states at all even f, $f=0$, and $f=\pm1$, in accordance with experiment.[8] Here the filling factor is $f=2\pi N/B$, with N as the number of electrons measured from a half-filled band. This still, however, leaves a complete freedom of choice of the vector (a,b,c). In particular, this choice may differ for the two spin states as well. For example, at $B=0$ and at strong V, one expects the interactions to prefer $a=1$ for both projections of spin—i.e., the CDW.[2] For strong U and at $B=0$, on the other hand, it is $a=\sigma$—i.e., the AF—that has lower energy.[7] $a=0$ would correspond to the competing "Kekule" ordering.[16] Which direction on the chiral manifold is actually chosen by the system is thus obviously a question of dynamics, to which we turn next.

The low-energy Lagrangian for the extended Hubbard model may be written as[7]

$$L = i\sum_\sigma \bar{\Psi}_\sigma\gamma_\mu D_\mu\Psi_\sigma - \sum_\sigma (r+\sigma g_zB)\Psi_\sigma^\dagger\Psi_\sigma - g_c\left(\sum_\sigma \bar{\Psi}_\sigma\Psi_\sigma\right)^2 - g_a\left(\sum_\sigma \sigma\bar{\Psi}_\sigma\Psi_\sigma\right)^2, \tag{9}$$

where $\bar{\Psi}_\sigma=\Psi_\sigma^\dagger(\vec{x},\tau)\gamma_0$, $D_0=-i\partial_\tau$, with τ as the imaginary time, $\mu=0,1,2$, and $\gamma_0=I_2\otimes\sigma_z$, $\gamma_1=\sigma_z\otimes\sigma_y$, and $\gamma_2=I_2\otimes\sigma_x$. Here $g_a\approx Ua^2/8$, $g_c\approx(3V-U)a^2/8$, g_z is the (dimensionless) effective g factor of the electron, and $B=(B_\perp^2+B_\parallel^2)^{1/2}$, with $B_\parallel$ as the field's in-plane component. We have retained only the *two least irrelevant* short-range interactions among those present in the full effective Lagrangian at $B=0$.[7] This will prove justified at the magnetic fields of interest, as discussed shortly. We have also set the mass of the electron m_e to unity.

Performing the Hubbard-Stratonovich transformation and neglecting the quantum fluctuations the free energy per unit area and at $T=0$ may be written as

$$F(m_c,m_a) - F(0,0) = \frac{m_c^2}{4g_c} + \frac{m_a^2}{4g_a} + \frac{B_\perp}{4\pi^{3/2}} \int_0^\infty \frac{ds}{s^{3/2}} \sum_{\sigma=\pm} (e^{-sm_\sigma^2} - 1) f_\sigma(s,m_\sigma), \tag{10}$$

where $m_\sigma = m_c + \sigma m_a$ and the function

$$f_\sigma(s,m) = \theta(|m| - |r + \sigma g_z B|) + C(s\Lambda^2)(\coth(sB_\perp) - 1). \tag{11}$$

Here $m_c/g_c = \Sigma_\sigma \langle \bar{\Psi}_\sigma \Psi_\sigma \rangle$ and $m_a/g_a = \Sigma_\sigma \sigma \langle \bar{\Psi}_\sigma \Psi_\sigma \rangle$ are the CDW and AF order parameters,[7] respectively. $C(x)$ is the cutoff function that satisfies $C(x \to \infty) = 1$ and $C(x \to 0) = 0$. Summing over the LLs below a sharp cutoff in energy, for example, yields $C(x) = 1 - e^{-x}$. The first term in Eq. (11) represents the crucial zeroth LL contribution and the second the remaining LLs. Zeeman energy is taken to always be smaller than the separation between the zeroth and the first LL—i.e., $g_z B < \sqrt{2B_\perp}$.

Let us first consider the system at $r=0$. The free energy is minimized by the solution of

$$\frac{m_+}{g_+} + \frac{m_-}{g_-} = \frac{4B_\perp m_+}{\pi^{3/2}} \int_0^\infty \frac{ds}{s^{1/2}} e^{-sm_+^2} f_+(s,m_+), \tag{12}$$

$$\frac{m_-}{g_+} + \frac{m_+}{g_-} = \frac{4B_\perp m_-}{\pi^{3/2}} \int_0^\infty \frac{ds}{s^{1/2}} e^{-sm_-^2} f_-(s,m_-), \tag{13}$$

where $g_\pm^{-1} = g_c^{-1} \pm g_a^{-1}$. Assume both g_c and g_a to be weak, $\Lambda g_{c,a} \ll 1$, and positive, and $g_c > g_a$, for example. There are then three types of solutions:

(i) If $m_+ \geqslant m_- > g_z B$, then $m_+ = m_-$—i.e., $m_a = 0$ and $m_c = 2g_c B_\perp/\pi$. This is the CDW. It exists when $g_c > \pi g_z B/2B_\perp$. For $g_a > g_c$, of course, one finds $m_c = 0$ and $m_a = 2g_a B_\perp/\pi$—i.e., the AF (Fig. 2). This, in particular, includes the case of the pure Hubbard model with $V=0$. The linear dependence on $B_\perp$ reflects the proportionality of either m to the degeneracy of the LLs.

(ii) For $g_z B > m_+ \geqslant m_-$ one finds a paramagnet with $m_c = m_a = 0$, unless the stronger coupling exceeds the $B=0$ critical value of $\pi/8\Lambda$, which lies outside the weak-coupling regime.

(iii) Finally, when $m_+ > g_z B > |m_-|$, the solution is $m_x = g_x B_\perp/\pi$, where $x = c, a$. Both the CDW and AF order parameters are finite, which would corresponds to a *ferrimagnet*. This solution exists for $g_c + g_a > \pi g_z B/B_\perp$ and $|g_c - g_a| < \pi g_z B/B_\perp$.

At weak coupling only the first term, representing the zeroth LL in Eq. (11), actually matters for the gap m. The second term would become important only at strong couplings, or in the limit $B_\perp \to 0$. Comparing the energies of the four possible solutions, we find only three stable phases represented in Fig. 2. All three have the filling factor $f=0$. Even if both g_c and g_a are positive it is always energetically favorable to open a single but larger gap that corresponds to the dominant coupling. The aforementioned ferrimagnet, which would have $f=1$, is thus never the minimum of the energy at $r=0$. This may also be understood as follows. At low magnetic fields, such that $l_B \gg a$ where $l_B = 1/\sqrt{B_\perp}$ is the magnetic length in our units, the flow of the couplings implied by the invariance of the gaps in Eqs. (12) and (13) with respect to change of the cutoff Λ, in the regime $\Lambda \gg 1/l_B$, is the same as at $B_\perp = 0$.[17] All weak couplings are thus irrelevant at intermediate length scales between the lattice constant and the magnetic length.[7] At $B_\perp \neq 0$ the flow of the interaction couplings towards the stable Gaussian fixed point is terminated at the cutoff $\sim 1/l_B$, with the least irrelevant coupling being left as dominant in the low-energy theory. This single surviving coupling then selects and generates the "relativistic" gap at $B_\perp \neq 0$. All other more irrelevant couplings can be neglected, as we partially did in Eq. (9), from the outset. Incidentally, this also justifies the Hartree approximation to the free energy utilized in Eq. (10): as long as the ground state is semimetallic and gapless at $B_\perp = 0$, for a weak enough magnetic field the low-energy theory at the cutoff $\sim 1/l_B \ll 1/a$ is indeed weakly interacting, as assumed.

It is useful to display explicitly the relevant energy scales in the problem. First, the relativistic gap is $m \approx (U/8) \times (B_\perp/B_0)$, where $B_0 = 1/a^2 \approx 10^5$ T is the characteristic scale for the magnetic field set by the lattice constant. Assuming $U \approx 10$ eV gives $m \approx 1$ meV for $B_\perp \sim 10$ T. The LL separation, on the other hand, is $D_L \approx t(B_\perp/B_0)^{1/2}$ and thus by roughly two orders of magnitude larger. The Zeeman energy, on the other hand, for $g_z \approx 1$ is $D_z \approx (B/10^4\ \mathrm{T})$ eV and thus of a similar size as m. Since the widths of the plateaus at $f = 0, \pm 1, \pm 4$ are proportional to either m or D_z, both much smaller than D_L, this would naturally explain why these QH states require higher magnetic fields to become discernible in presence of some fixed disorder-induced broadening of the LLs.

The above discrepancy between the kinetic and the interaction energy scales is only the first in a general hierarchy of energy scales that is implied by the stability of the semimetallic fixed point at zero magnetic field. As discussed above, the magnetic field affects the flow of the interaction couplings only at the length scales above the magnetic length l. The development of an order parameter m_x in some channel may be understood as the divergence of the corresponding coupling constant x at the length scale $L_x = 1/m_x \gg l$. This is determined by x, via essentially dimensional analysis, by the relation $m_x l \approx x l^{-n}$, where $x l^{-n}$ is the dimensionless coupling, with $1/l$ now playing the role of the ultraviolet cutoff. For $x=g$ and $n=1$ this way we reproduce the above relation for the interaction gap m, and for $x=t$ and $n=0$ we get the characteristic kinetic energy scale D_L. The crucial point is that more irrelevant interactions at $B=0$, with higher negative dimensions n, translate at $B \neq 0$ into energy scales that depend on higher powers of B/B_0: $m_x \sim (B/B)^{(n+1)/2}$. In particular, this is what justifies the replacement of a realistic finite-range interaction with the simpler δ function in Eq. (9).

At $r=0$ there are thus two fundamentally different ground states: one at larger interactions that breaks the A-B sublattice symmetry, either in the charge (CDW) or the spin (AF) channel, with vanishing magnetization, and the other magnetic, at weaker interactions, with the full translational sym-

metry of the lattice. Both are incompressible and yield the plateau in the Hall conductivity at $f=0$. If the parameters are such to place the system for $B_\parallel=0$ into the former, increasing $B_\parallel$ would eventually cause the transition into the latter state. This certainly holds for the CDW, as well as for the AF with its Néel order directed along the magnetic field, as we assumed here.[18]

Hereafter, we will thus retain only the larger quartic coupling, call it g_x, and its corresponding order parameter in Eq. (10), m. At small m the free energy then becomes

$$\Delta F = \frac{m^2}{4g_x}[1 + O(\Lambda g_x)] + O(m^4) - \frac{B_\perp |m|}{2\pi}[\theta(|m| - |r + D_z|) + \theta(|m| - |r - D_z|)], \quad (14)$$

where $D_z = g_z B$. The nonanalytic term $\sim|m|$ comes from the zeroth LL. In the weak-coupling regime possible local minima are then at $m/m_0 = 0, 1/2, 1$, with $m_0 = 2g_x B_\perp/\pi$. Determination of the global minimum of the free energy at a finite chemical potential then leads to the phase diagram presented in Fig. 1. Let us determine the filling factor when $m = m_0/2$ solution is stable—i.e., in the strip $r + D_z > m_0$ and $|r - D_z| < m_0/2$ in Fig. 1. From the first inequality we see that $r + D_z > m$, and thus $r > m - D_z > -m - D_z$, so the values of two out of four spin- and sublattice-degeneracy-resolved energies of the zeroth LLs lie below the chemical potential. The second inequality implies that between the two remaining energies one is above and the other below the chemical potential. To see this, first assume $r > D_z$. Then $D_z - m < r < D_z + m$, as announced. If $r < D_z$, on the other hand, $D_z + m > r > D_z - m$ again, so in either case $f=1$. The determination of the filling factor for the remaining states is even simpler and follows analogously.

For $f \geqslant 2$ the relativistic gap is $m=0$, and there is a direct transition between $f=0$ to $f=2$ at $D_z/m_0 < 1/4$. For a fixed and larger D_z, by increasing the chemical potential the system always passes through the intermediate $f=1$ QH state, which is magnetic and breaks the discrete sublattice symmetry. The width of $f=1$ state is $2D_z - (m_0/2)$ for $D_z/m_0 < 3/4$, or m_0 for $D_z/m_0 > 3/4$. All transitions are discontinuous. As the ratio D_z/m_0 can be changed by varying $B_\parallel$, it follows that at a large enough $B_\parallel$ the width and the activation energy of the $f = \pm 1$ state become $\sim B_\perp$ and independent of $B_\parallel$, which should be experimentally testable. Since in the experiment[8] the width of the plateau at $f=0$ appears to be somewhat larger than at $f = \pm 1$ and $f = \pm 4$, the latter being always $2D_z$, we speculate that $1/4 < D_z/m_0 < 1/2$. If this is indeed the case, the activation energy at $f=0$ should first decrease before increasing with $B_\parallel$, whereas that of $f=1$ would increase and saturate.

The mechanism of "magnetic catalysis" of the 'relativistic' gap[9] utilized here has also been considered recently as an explanation of the integer QH effect in graphene in Ref. 12. The crucial difference from the present work is that only $\sim 1/r$ tail of the Coulomb interaction was included, which could produce only the CDW, and that with the large gap $m \sim \sqrt{B_\perp} \sim D_L$. To have m much smaller from the LL separation, as observed experimentally, requires then what appears to be an unrealistically strong screening of the Coulomb interaction by the substrate.[12] In this theory the gap is also always inhibited by a finite chemical potential and thus cannot exist at $f=1$ if it did not already at $f=0$. This would imply that the activation gap in Ref. 12 at $f=1$ is always the Zeeman energy. Both results are in sharp contradiction with ours.

The QH effect in graphene was also recently discussed in Ref. 13. The principal difference from the present work is that the AF ordering was entirely neglected, so that the existence of the QH state at $f=1$ in Ref. 13 is always due to the CDW, which then requires a large enough V. In contrast, in the present theory $f=1$ state can exist even for $V=0$ when it is due to the AF ordering. In particular, setting $V = g_z = 0$ we find the pure ($V=0$) weakly coupled Hubbard model at half filling and in magnetic field to be an AF, and not the Stoner's ferromagnet, as assumed in Ref. 13. This is because a finite AF order parameter, unlike the magnetization, besides splitting the zeroth LL, also lowers the energy of all other occupied LLs. Put differently, in considering the dynamics within only the zeroth LL, the couplings need to be renormalized up to the length scale of the magnetic length l_B first. Then $g_a(l_B) \gg g_f(l_B)$ always, where g_f is the coupling in the ferromagnetic channel,[7] for this reason omitted in Eq. (9). Retaining such a ferromagnetic coupling may be shown to only increase the activation energy when $m=0$ to $D_z + 2g_f B_\perp/\pi$.

CDW formation due to lattice distortion has been proposed as a mechanism behind the QH effect in graphene in Ref. 14. This explanation differs from the present and all the other ones in that Coulomb repulsion plays essentially no role in it. In particular, an $f=1$ incompressible state would in that scenario appear with increase of the chemical potential for any Zeeman energy, in contrast to our Fig. 1, where for weak Zeeman energy there is a direct transition from $f=0$ to $f=2$.

Finally, the present mechanism differs essentially from the recent proposal[15] in which disorder is invoked to explain the absence of QH states at odd $f \neq \pm 1$.

In this paper we have neglected entirely the effect of disorder. As usual, it will broaden the LLs and thus provide an intrinsic energy scale that needs to be exceeded in order for an incompressible state to be resolved. We believe that this is why the states at $f=0$, $f = \pm 1$, and $f = \pm 4$ become visible only at higher fields than the main sequence at $f = 4n+2$, since their energy gaps according to our scenario are inherently smaller. They may be therefore understood as the *fine structure* of the QH effect in graphene.

To summarize, we assumed that the principal effect of the Coulomb interaction in graphene is to introduce the on-site and nearest-neighbor repulsion for electrons on a honeycomb lattice. Postulating further a semimetallic ground state in zero field, we argued that at a finite field there exists a hierarchy of energy scales, determined by the degrees of irrelevancy of the corresponding couplings at $B=0$. In this work we considered only the effects of the least irrelevant interaction, which we expect to give the leading correction to the Landau level structure for the noninteracting electrons. The phase diagram of graphene at laboratory magnetic fields ~ 10 T is proposed. The theory predicts the incompressible states at all even integer filling factors including $f=0$, and at

$f=\pm 1$. The ground state of the system at $f=0$ either breaks the sublattice symmetry, in either charge or spin channels, or is magnetic, depending on the magnitude of the Zeeman energy. At $f=\pm 1$ the system is always in the translational symmetry-breaking phase and with finite magnetization, whereas at $|f| \geqslant 2$ the sublattice symmetry is preserved. The phase diagram in the Zeeman energy-chemical potential plane is proposed, and several of its features that may be used to distinguish the present from other proposed scenarios are discussed.

The author is grateful to J. Alicea, J.-N. Fuchs. V. Gusynin, and S. Sharapov for useful discussions and correspondence. This work was supported by the NSERC of Canada.

[1] P. K. Wallace, Phys. Rev. **71**, 622 (1947).
[2] G. W. Semenoff, Phys. Rev. Lett. **53**, 2449 (1984).
[3] K. S. Novoselov, A. K. Geim, S. V. Morozov, D. Jiang, M. I. Katsnelson, I. V. Grigorieva, S. V. Dubonos, and A. A. Firsov, Nature (London) **438**, 197 (2005).
[4] Y. Zhang, Y.-W. Tan, H. L. Stormer, and P. Kim, Nature (London) **438**, 201 (2005).
[5] V. P. Gusynin and S. G. Sharapov, Phys. Rev. Lett. **95**, 146801 (2005); N. M. R. Peres, F. Guinea, and A. H. Castro Neto, Phys. Rev. B **72**, 174406 (2005).
[6] D. V. Khveshchenko, Phys. Rev. Lett. **87**, 246802 (2001).
[7] I. F. Herbut, Phys. Rev. Lett. **97**, 146401 (2006).
[8] Y. Zhang, Z. Jiang, J. P. Small, M. S. Purewal, Y.-W. Tan, M. Fazlollahi, J. D. Chudow, J. A. Jaszczak, H. L. Stormer, and P. Kim, Phys. Rev. Lett. **96**, 136806 (2006).
[9] V. P. Gusynin, V. A. Miransky, and I. A. Shovkovy, Phys. Rev. Lett. **73**, 3499 (1994); Phys. Rev. D **52**, 4718 (1995).
[10] fA. L. Tchougreeff and R. Hoffmann, J. Phys. Chem. **96**, 8993 (1992).
[11] See also I. F. Herbut, Phys. Rev. Lett. **88**, 047006 (2002); Phys. Rev. B **66**, 094504 (2002), for analogous chiral symmetry of *d*-wave superconductors.
[12] V. P. Gusynin, V. A. Miransky, S. G. Sharapov, and I. A. Shovkovy, Phys. Rev. B **74**, 195429 (2006).
[13] J. Alicea and M. P. A. Fisher, Phys. Rev. B **74**, 075422 (2006).
[14] J.-N. Fuchs and P. Lederer, Phys. Rev. Lett. **98**, 016803 (2007).
[15] K. Nomura and A. H. MacDonald, Phys. Rev. Lett. **96**, 256602 (2006).
[16] C-Y. Hou, C. Chamon, and C. Mudry, arXiv:cond-mat/0609740 (unpublished).
[17] See K. Kaveh and I. F. Herbut, Phys. Rev. B **71**, 184519 (2005), for such an alternative derivation of the renormalization group flow.
[18] Allowing the staggered magnetization to point in other spatial directions diminishes the competition between the Néel order and Zeeman term [I. F. Herbut (unpublished)].